

# Dissociation of SO<sub>2</sub> on Au/TiC(001): Effects of Au–C Interactions and Charge Polarization\*\*

José A. Rodríguez,\* Ping Liu, Francesc Viñes, Francesc Illas, Yoshiro Takahashi, and Kenichi Nakamura

Recently, gold has become the subject of much attention due to its unusual catalytic properties when dispersed on some oxide supports (TiO<sub>2</sub>, CrO<sub>x</sub>, MnO<sub>x</sub>, Fe<sub>2</sub>O<sub>3</sub>, Al<sub>2</sub>O<sub>3</sub>, MgO).<sup>[1–9]</sup> Bulk metallic gold has low reactivity as a consequence of a combination of a deep-lying valence d band and very diffuse valence s,p orbitals.<sup>[10]</sup> Several models have been proposed for explaining the activation of supported gold: From special chemical properties resulting from the small size of the active gold particles (usually less than 5 nm),<sup>[1,3–5]</sup> to the effects of charge transfer between the oxide and gold.<sup>[2,3,6,7]</sup> What happens when Au is deposited on a substrate which has physical and chemical properties that differ from those of an oxide? The carbides of the early transition metals exhibit, in many aspects, chemical behavior similar to that of noble metals.<sup>[11]</sup> A recent article indicates that Au particles (ca. 2 nm in size) dispersed on TiC can oxidize carbon monoxide (CO + 0.5 O<sub>2</sub> → CO<sub>2</sub>) at temperatures below 200 K.<sup>[12]</sup> What is the nature of the Au–TiC interactions? In this work we investigate the adsorption of SO<sub>2</sub> on well-defined Au/TiC(001) surfaces using synchrotron-based high-resolution photoemission and first-principles DFT calculations. Sulfur dioxide is an excellent probe molecule for determining the reactivity of gold in different chemical environments,<sup>[13–15]</sup> and its dissociation is a much more demanding reaction than the oxidation of CO.<sup>[14]</sup> The destruction of SO<sub>2</sub> (DeSOx) is a very important problem in environmental chemistry due to the adverse effects of acid rain (the main product of the oxidation of SO<sub>2</sub> in the atmosphere) on the environment and corrosion of monuments and buildings.<sup>[16,17]</sup> As we show below, Au/TiC has

much higher DeSOx activity than Au supported on oxide surfaces or pure TiC. This is, in part, a consequence of charge polarization around gold induced by Au–C interactions.

Figure 1 shows S 2p photoemission spectra recorded after dosing five Langmuir (L) of SO<sub>2</sub> to pure TiC(001) at 150 and 300 K. In agreement with previous studies,<sup>[18,19]</sup> molecular

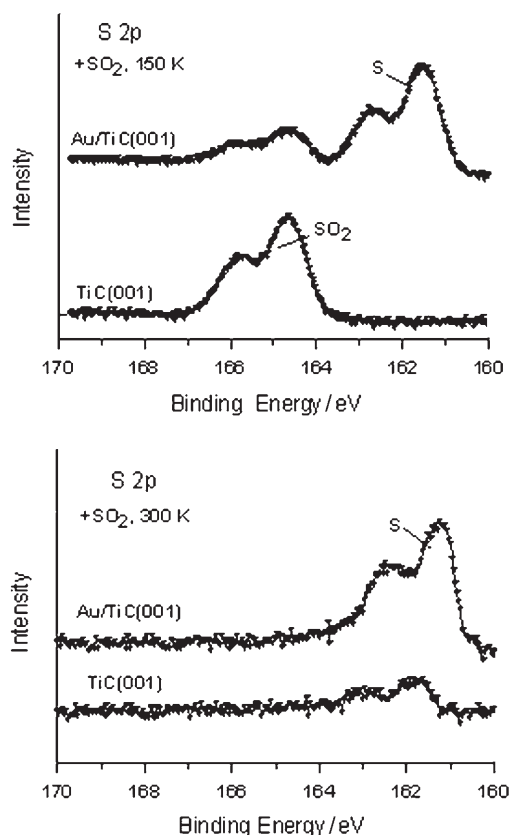


**Figure 1.** S 2p spectra collected after dosing 5 L of SO<sub>2</sub> to TiC(001) and to a surface precovered with 0.2 ML of gold. SO<sub>2</sub> was dosed at 150 (top panel) and 300 K (bottom panel). A photon energy of 380 eV was used to excite the electrons.

chemisorption is seen at 150 K and some dissociative chemisorption—SO<sub>2</sub>(gas) → S(ads) + 2 O(ads)—at 300 K. In general terms, TiC(001) can be classified as a poor DeSOx system.<sup>[18]</sup> Au(111) and polycrystalline gold also interact weakly with SO<sub>2</sub> and are not efficient for the dissociation of S–O bonds.<sup>[20]</sup> However, after depositing 0.2 monolayers (ML) of Au on TiC(001) the reactivity of the system drastically increases. In Figure 1, the S 2p spectrum recorded

[\*] Dr. J. A. Rodríguez, Dr. P. Liu  
Chemistry Department  
Brookhaven National Laboratory, Upton, NY 11973 (USA)  
Fax: (+1) 631-344-5815  
E-mail: rodriguez@bnl.gov

F. Viñes, Prof. F. Illas  
Departament de Química Física & IQTCUB  
Universitat de Barcelona  
C/Martí i Franquès 1, 08028 Barcelona (Spain)

Y. Takahashi, Prof. K. Nakamura  
Materials and Structures Laboratory  
Tokyo Institute of Technology, Yokohama 226-8503 (Japan)

[\*\*] The research carried out at BNL was supported by the US Department of Energy, Chemical Sciences Division. J.A.R. acknowledges the support of the Generalitat de Catalunya in a visit to the Universitat de Barcelona. F.V. thanks the Spanish Ministry of Education and Science and Universitat de Barcelona for supporting his predoctoral research. K.N. thanks the Nippon Foundation for Materials Science for grants that made possible part of this work. Computational time on the Marenostrum supercomputer of the Barcelona Supercomputing Center is gratefully acknowledged.

after dosing  $\text{SO}_2$  to Au/TiC(001) at 150 K shows enhanced uptake of the compound with respect to clean TiC(001) and, more importantly, full dissociation of the S–O bonds occurs. At 150 K, the features of atomic S dominate the S 2p spectrum for  $\text{SO}_2/\text{Au}/\text{TiC}(001)$  with a small contribution from adsorbed  $\text{SO}_2$ . If dosing of  $\text{SO}_2$  is done at 300 K, only adsorbed S is detected.

Figure 2 shows Au 4f spectra recorded before and after adsorbing  $\text{SO}_2$  at 150 K on a TiC(001) surface precovered with Au. The Au 4f<sub>7/2</sub> peak of Au/TiC(001) appears at a binding energy of about 84.1 eV, which is somewhat larger than the

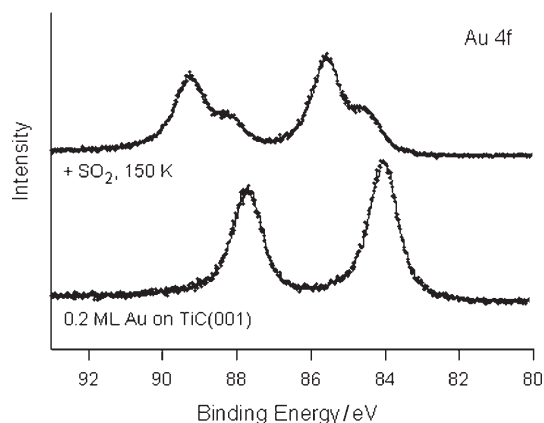


**Figure 2.** Au 4f spectra collected before and after dosing 5 L of  $\text{SO}_2$  to a TiC(001) surface precovered with 0.2 ML of gold.  $\text{SO}_2$  was dosed at 150 K. A photon energy of 380 eV was used to excite the electrons.

value of 83.8 eV measured for bulk gold. Au grows on TiC(001) to form three-dimensional islands and exhibits electronic perturbations.<sup>[21]</sup> Adsorption of  $\text{SO}_2$  on Au/TiC(001) substantially modifies the Au 4f features. These can be fitted<sup>[13–15]</sup> by a set of two doublets with 4f<sub>7/2</sub> binding energies of 84.6 and 85.4 eV. The doublet at lower binding energy may be due to chemisorption of S or O on the Au nanoparticles, while the doublet at higher binding energy suggests formation of  $\text{Au}_x\text{S}$  or  $\text{Au}_y\text{O}$  compounds.<sup>[22]</sup> These results indicate that Au participates directly in dissociation of the  $\text{SO}_2$  molecule. The inert behavior seen for Au(111) or polycrystalline gold<sup>[20]</sup> has disappeared.

Carbon 1s spectra for clean TiC(001), Au/TiC(001), and  $\text{SO}_2/\text{Au}/\text{TiC}(001)$  are displayed in Figure 3. Our spectrum of TiC(001) matches well that reported in reference [23]. Deposition of Au substantially increases the full width at half-maximum (FWHM) of the C 1s peak. Density functional calculations indicate that this change in line shape is due to formation of Au–C bonds.<sup>[21]</sup> For Au on TiC(001), the strongest bonding interactions are observed when the Au atoms are above carbon sites, and the weakest for bonding above titanium sites. The dissociative adsorption of  $\text{SO}_2$  on Au/TiC(001) at 150 K or higher leads to the appearance of new C 1s features at binding energies of 282–284 eV. This is accompanied by a shift of about 0.35 eV in the peak position of the Ti 2p<sub>3/2</sub> peak and a minor increase (ca. 0.2 eV) in its FWHM. Comparison with the C 1s and Ti 2p spectra of O/

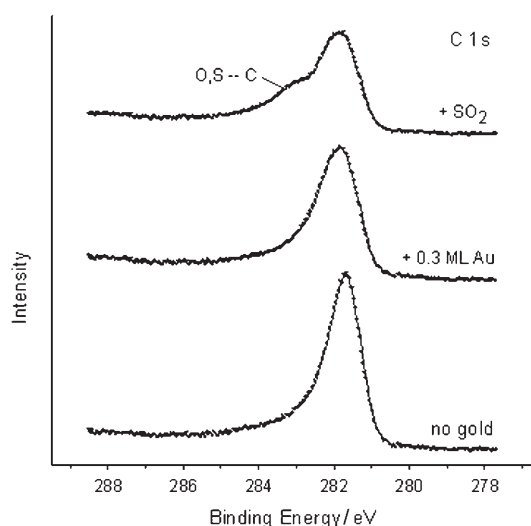


**Figure 3.** C 1s photoemission data for clean TiC(001) and an Au/TiC(001) surface before and after adsorbing  $\text{SO}_2$  at 150 K. A photon energy of 380 eV was used to excite the electrons.

TiC(001)<sup>[24]</sup> and S/TiC(001)<sup>[25]</sup> indicates that the S and O atoms produced in the DeSOx process bind to the C and Ti sites of the carbide substrate. Indeed, the DFT calculations discussed below show unequivocally that these surface sites are essential in the energetics for the cleavage of S–O bonds.

The photoemission data reveal that Au/TiC(001) is a much better DeSOx system than either Au/MgO(100)<sup>[14]</sup> or Au/TiO<sub>2</sub>(110).<sup>[13]</sup> Gold particles dispersed on MgO(100) can perform oxidation of CO<sup>[4]</sup> and bind  $\text{SO}_2$  more strongly than extended surfaces of gold,<sup>[20]</sup> but the Au/MgO(100) system cannot dissociate the  $\text{SO}_2$  molecule, which is desorbed intact when the temperature is raised from 150 to 270 K.<sup>[14]</sup> In the case of Au particles supported on TiO<sub>2</sub>(001),  $\text{SO}_2$  is adsorbed molecularly at 150 K and dissociates on heating to room temperature.<sup>[13]</sup> Au/TiC(001) can break both S–O bonds at a temperature as low as 150 K. Figure 4 compares the amount of atomic sulfur adsorbed after exposing Au/MgO(100),<sup>[14]</sup> Au/TiO<sub>2</sub>(110),<sup>[13]</sup> and Au/TiC(001) to 5 L of  $\text{SO}_2$  at 300 K. Under these conditions the amount of  $\text{SO}_2$  that dissociates on Au/MgO(100) is negligible.<sup>[14]</sup> The deposition of Au on TiO<sub>2</sub>(110) produces surfaces quite active for the destruction of  $\text{SO}_2$ .<sup>[13]</sup> In Figure 4, Au/TiC(001) displays a higher DeSOx activity than Au/TiO<sub>2</sub>(110) even at high Au loads. Scanning tunneling microscopy (STM) images of Au/TiC(001) point to a very high DeSOx activity when the Au particles are smaller than 1.5 nm. The DeSOx activity of Au/TiC(001) decreases substantially when the Au particle size exceeds 2 nm at Au coverages higher than 1 ML. Small Au clusters are essential for high DeSOx activity.

We examined the mechanism for the dissociation of  $\text{SO}_2$  on Au/TiC(001) using DFT. Experiments<sup>[20]</sup> and DFT calculations show very weak bonding interactions between  $\text{SO}_2$  and either Au(111) or Au(100). Using different GGA functionals (RPBE, PW91, Becke-88/Perdew-91), we found a binding energy of less than 0.15 eV for different configurations of  $\text{SO}_2$  on Au(111) and Au(100). What is the intrinsic reactivity of Au

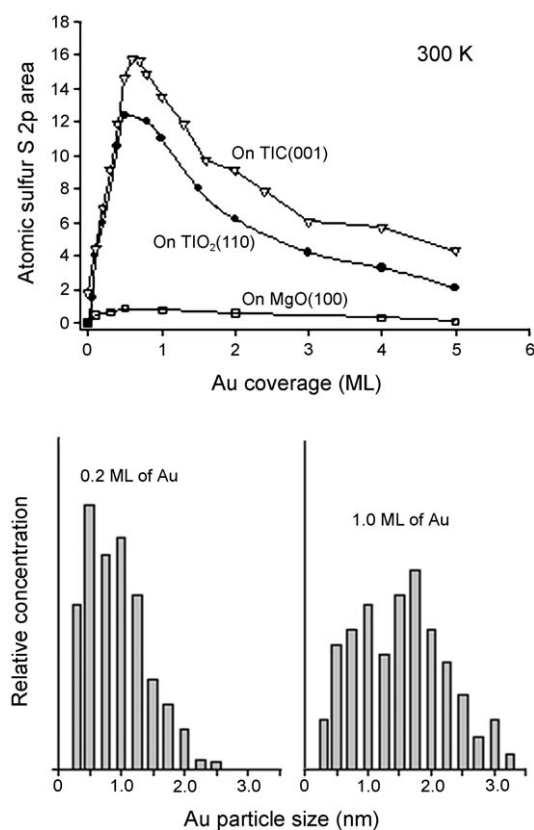


**Figure 4.** Top: Effect of Au coverage on the amount of atomic S deposited on Au/MgO(001),<sup>[14]</sup> Au/TiO<sub>2</sub>(110),<sup>[13]</sup> and Au/TiC(001) after dosing 5 L of SO<sub>2</sub> at 300 K. Bottom: Distribution of Au particle sizes determined from STM images recorded after depositing 0.2 and 1.0 ML of Au on TiC(001) at 300 K.

nanoparticles or clusters towards SO<sub>2</sub>? We examined the bonding of SO<sub>2</sub> to a series of free, unsupported Au clusters: Au, Au<sub>2</sub>, Au<sub>3</sub>, Au<sub>4</sub>, Au<sub>13</sub>, and Au<sub>29</sub>. The geometry of these clusters was either optimized for the gas phase (Au<sub>2</sub>, Au<sub>3</sub>, and Au<sub>4</sub>)<sup>[27]</sup> or detected by electron microscopy (Au<sub>13</sub> and Au<sub>29</sub>).<sup>[8,28]</sup> The bonding energy of SO<sub>2</sub> to the Au clusters was in the range of 0.7–1.5 eV (RPBE functional) and 0.9–1.8 eV (PW91 and Becke-88/Perdew-91 functionals). Two factors contribute to the special reactivity of the Au clusters. First, they contain Au atoms that have a relatively low coordination number.<sup>[28,29]</sup> Second, the Au clusters can exhibit a high degree of fluxionality and adapt their morphology in the presence of an adsorbate.<sup>[4,28]</sup> Although the Au clusters bind SO<sub>2</sub> much better than Au(111) and Au(100), they are not yet able to dissociate its S–O bonds. The SO<sub>2</sub>(ads)→S(ads)+2O(ads) reaction has a large activation barrier (>1 eV) on the free gold clusters, and in many cases it is an endothermic process. Thus, Au–TiC(001) interactions play a key role in the dissociation of SO<sub>2</sub>.

A previous theoretical study indicates that Au, Au<sub>2</sub>, Au<sub>3</sub>, and Au<sub>4</sub> prefer to be adsorbed on carbon sites of TiC(001).<sup>[21]</sup> We found the same after deposition of Au<sub>13</sub> or Au<sub>29</sub> on TiC(001); see Figure 5. The square lattice of the carbide substrate forces a square-pyramidal shape on the supported

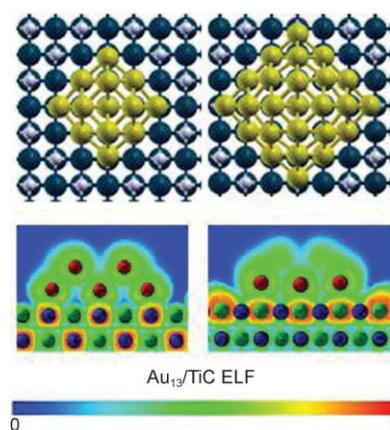


**Figure 5.** Top: Bonding configurations for Au<sub>13</sub> and Au<sub>29</sub> on TiC(001). Gold atoms are shown as yellow spheres, Ti atoms as blue spheres, and C atoms as gray spheres. Au<sub>13</sub> consists of two layers of 9 and 4 metal atoms. Au<sub>29</sub> contains three layers of 16, 9, and 4 Au atoms.<sup>[8,28]</sup> Bottom: ELF maps for Au<sub>13</sub> on TiC(001). The left panel shows a cut along the diagonal of the cluster in a plane which contains gold atoms. A cut across the center (joining two faces) in a plane which contains three gold atoms is displayed in the right panel. The probability of finding the electron varies from 0 (blue) to 1 (red).

Au<sub>13</sub> and Au<sub>29</sub> clusters. We have also seen this particle shape in STM images of Au/TiC(001) surfaces. The electronic structure of the Au/TiC(001) systems was examined through a topological analysis of the electron localization function (ELF),<sup>[30]</sup> and charge distributions were estimated by the method of Bader.<sup>[31]</sup> A Bader analysis of the electron density showed a very small net charge transfer from the surface to the gold clusters ( $Q_{Au} < 0.2 e$ ). Figure 5 displays ELF plots for Au<sub>13</sub> on TiC(001). After adsorption of the metal cluster, redistribution of charge occurs in the carbide and around the adatoms. The net result is a substantial concentration of electrons in the region outside Au<sub>13</sub>, especially for the metal atoms in contact with the carbide substrate. A similar phenomenon was observed for adsorbed Au, Au<sub>2</sub>, and Au<sub>4</sub>,<sup>[21]</sup> and the magnitude of the polarization was larger for the small Au particles. The polarization of charge around gold is quite interesting, because it should facilitate bonding with SO<sub>2</sub><sup>[13–15]</sup> or other electron-acceptor molecules (CO, O<sub>2</sub>, C<sub>2</sub>H<sub>4</sub>, C<sub>2</sub>H<sub>2</sub>, etc.).

Figure 6 shows the calculated adsorption energy for SO<sub>2</sub> on clean TiC(001) and on carbide surfaces with Au atoms, Au<sub>4</sub>, or Au<sub>13</sub> clusters, an Au wire, and a flat Au monolayer. All the Au/TiC(001) surfaces bond SO<sub>2</sub> more strongly than clean TiC(001) or the corresponding isolated Au system. Spontaneous dissociation was observed when the SO<sub>2</sub> was set at gold/carbide interfaces. Thus, supported Au atoms, Au<sub>4</sub>, Au<sub>13</sub>, and an Au wire worked in a cooperative way with the carbide and dissociated S–O bonds. The photoemission results in Figures 2 and 3 also indicate direct participation of Au, Ti, and C sites in S–O bond cleavage. Figure 6 shows that an ideal flat monolayer of gold bonded to TiC(001) adsorbs SO<sub>2</sub> much more strongly than Au(111) or Au(100), but it is not able to dissociate the adsorbate due to the lack of a gold/carbide interface. The DFT calculations corroborate that the size of

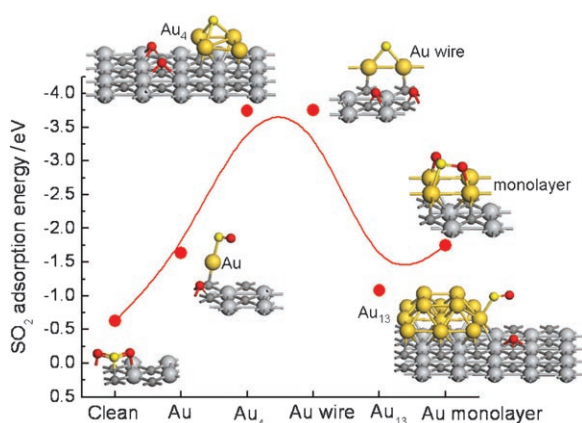


**Figure 6.** Calculated adsorption energies (RPBE, DMol<sup>3</sup>) and bonding configurations for SO<sub>2</sub> on TiC(001) and Au/TiC(001). Au is shown as large yellow spheres, Ti as large gray spheres, C as small gray spheres, S as small yellow spheres, and O as small red spheres. Au atoms, Au<sub>4</sub> and Au<sub>13</sub> clusters, an Au wire, and a flat Au monolayer were deposited on TiC(001). SO<sub>2</sub> was initially set at the gold/carbide interface and, in most cases, spontaneously dissociated during geometry optimization.

the Au particle has a drastic effect on the reactivity of the system. Supported Au<sub>29</sub> displayed much lower DeSOx activity than supported Au<sub>4</sub> or Au<sub>13</sub>, and no dissociation of SO<sub>2</sub> was observed. The effects of the Au–TiC(001) interactions are significant only for small Au particles. Our studies show that this is also valid for oxidation of CO, reduction of NO, and the water-gas shift reaction. In the case of CO oxidation, good catalytic activity is observed after depositing Au particles of 2 nm on a TiC film,<sup>[12]</sup> and the catalytic activity improves substantially when small Au particles (< 1 nm) are supported on TiC(001).

In summary, our experimental and theoretical studies show that Au/TiC(001) has extremely high DeSOx activity, and is more efficient for this process than either Au/MgO(100) or Au/TiO<sub>2</sub>(110). Special electronic and new chemical properties can be obtained by depositing small Au particles on a metal carbide substrate. The Au–TiC bond has little ionic character but substantial redistribution of electrons takes place. The polarization of charge around gold facilitates bonding of the adatoms with electron-acceptor molecules and produces systems with high chemical and catalytic activity.

## Experimental Section

The photoemission studies were performed at the U7A beamline of the National Synchrotron Light Source at Brookhaven National Laboratory.<sup>[13–15]</sup> A photon energy of 380 eV was used to acquire the C1s, S2p, and Au4f spectra, while a photon energy of 550 eV was utilized to collect the Ti2p data. Experiments were also performed at two ultrahigh-vacuum chambers located at the Tokyo Institute of Technology with capabilities for X-ray photoelectron spectroscopy (AlK<sub>α</sub> X-ray source), low-energy electron diffraction, thermal desorption mass spectroscopy, and scanning tunneling microscopy.<sup>[18,21]</sup> The Au/TiC(001) surfaces were prepared by following the methodology described in the literature.<sup>[21]</sup> SO<sub>2</sub> (99.98% purity) was dosed through gas-capillary arrays positioned near the samples.<sup>[13–15]</sup> The gas exposures are based on ion-gauge readings and are not corrected for capillary-array enhancement.

The DFT calculations were performed with the VASP or DMol<sup>3</sup> codes, as detailed in references [19,21]. VASP was used to investigate the nature of the Au–TiC(001) interactions.<sup>[21]</sup> It uses a plane-wave basis set. The atomic cores are represented by the projected augmented plane-wave method of Blöchl. The VASP calculations were done with the PW91 form of the generalized gradient approximation for the exchange correlation. The bonding of SO<sub>2</sub> to Au clusters and Au/TiC(001) was examined with DMol<sup>3</sup> including all the electrons and relativistic effects.<sup>[14,19]</sup> The DMol<sup>3</sup> calculations used numerical basis sets and the RPBE, PW91, or Becke-88/Perdew-91 descriptions of the exchange and correlation functionals. Slabs of four atomic layers were utilized to model the TiC(001) substrate.<sup>[19,21]</sup> During the DFT calculations the geometries of the first layer of TiC and the Au adatoms were allowed to fully relax together with SO<sub>2</sub>.

Received: March 3, 2008

Revised: May 13, 2008

Published online: July 16, 2008

**Keywords:** carbides · density functional calculations · desulfurization · gold · surface chemistry

- [1] M. Haruta, *Catal. Today* **1997**, *36*, 153.
- [2] M. S. Chen, D. W. Goodman, *Science* **2004**, *306*, 252.
- [3] C. T. Campbell, *Science* **2004**, *306*, 234.
- [4] H. Häkkinen, S. Abbet, A. Sanchez, U. Heiz, U. Landman, *Angew. Chem.* **2003**, *115*, 1335; *Angew. Chem. Int. Ed.* **2003**, *42*, 1297.
- [5] I. N. Remediakis, N. Lopez, J. K. Nørskov, *Angew. Chem.* **2005**, *117*, 1858; *Angew. Chem. Int. Ed.* **2005**, *44*, 1824.
- [6] Q. Fu, H. Saltsburg, M. Flytzani-Stephanopoulos, *Science* **2003**, *301*, 935.
- [7] A. Abad, P. Concepción, A. Corma, H. García, *Angew. Chem.* **2005**, *117*, 4134; *Angew. Chem. Int. Ed.* **2005**, *44*, 4066; M. Boronat, P. Concepción, A. Corma, S. González, F. Illas, P. Serna, *J. Am. Chem. Soc.* **2007**, *129*, 16230.
- [8] J. A. Rodríguez, P. Liu, J. Hrbek, J. Evans, M. Pérez, *Angew. Chem.* **2007**, *119*, 1351; *Angew. Chem. Int. Ed.* **2007**, *46*, 1329.
- [9] J. A. Rodríguez, S. Ma, P. Liu, J. Evans, M. Pérez, *Science* **2007**, *318*, 1757.
- [10] a) B. Hammer, J. K. Nørskov, *Adv. Catal.* **2000**, *45*, 71; b) J. A. Rodríguez, M. Kuhn, *Surf. Sci.* **1995**, *330*, L657.
- [11] H. Hwu, J. G. Chen, *Chem. Rev.* **2005**, *105*, 185.
- [12] a) L. K. Ono, B. Roldán-Cuenya, *Catal. Lett.* **2007**, *113*, 86; b) L. K. Ono, D. Sudfeld, B. Roldán-Cuenya, *Surf. Sci.* **2006**, *600*, 5041.
- [13] J. A. Rodríguez, G. Liu, T. Jirsak, J. Hrbek, Z. Chang, J. Dvorak, A. Maiti, *J. Am. Chem. Soc.* **2002**, *124*, 5242.
- [14] J. A. Rodríguez, M. Pérez, T. Jirsak, J. Evans, J. Hrbek, L. González, *Chem. Phys. Lett.* **2003**, *378*, 526.
- [15] J. A. Rodríguez, M. Peréz, J. Evans, G. Liu, J. Hrbek, *J. Chem. Phys.* **2005**, *122*, 241101.
- [16] A. C. Stern, R. W. Boubel, D. B. Turner, D. L. Fox, *Fundamentals of Air Pollution*, 2nd ed, Academic, Orlando, **1984**.
- [17] A. Pieplu, O. Saur, J.-C. Lavalley, O. Legendre, C. Nèdez, *Catal. Rev. Sci. Eng.* **1998**, *40*, 409.
- [18] J. A. Rodríguez, P. Liu, J. Dvorak, T. Jirsak, J. Gomes, Y. Takahashi, K. Nakamura, *Surf. Sci.* **2003**, *543*, L675.
- [19] P. Liu, J. A. Rodríguez, *J. Chem. Phys.* **2003**, *119*, 10895.
- [20] G. Liu, J. A. Rodríguez, J. Dvorak, J. Hrbek, T. Jirsak, *Surf. Sci.* **2002**, *505*, 295.
- [21] J. A. Rodríguez, F. Viñes, F. Illas, P. Liu, Y. Takahashi, K. Nakamura, *J. Chem. Phys.* **2007**, *127*, 211102.
- [22] X. Wang, J. A. Rodríguez, J. C. Hanson, M. Pérez, J. Evans, *J. Chem. Phys.* **2005**, *123*, 221101.



- [23] L. I. Johansson, H. I. P. Johansson, K. L. Håkansson, *Phys. Rev. B* **1993**, 48, 14520.
  - [24] J. A. Rodriguez, P. Liu, J. Dvorak, T. Jirsak, J. Gomes, Y. Takahashi, K. Nakamura, *J. Chem. Phys.* **2004**, 121, 465.
  - [25] J. A. Rodriguez, P. Liu, J. Dvorak, T. Jirsak, J. Gomes, Y. Takahashi, K. Nakamura, *Phys. Rev. B* **2004**, 69, 115414.
  - [26] M. Valden, X. Lai, D. W. Goodman, *Science* **1998**, 281, 1647.
  - [27] R. M. Olson, S. Varganov, M. S. Gordon, H. Metiu, S. Chretien, P. Piecuch, K. Kowalski, S. A. Kucharski, M. Musia, *J. Am. Chem. Soc.* **2005**, 127, 1049.
  - [28] L. Barrio, P. Liu, J. A. Rodriguez, J. M. Campos-Martin, J. L. G. Fierro, *J. Phys. Chem. C* **2007**, 111, 19001.
  - [29] A. Corma, M. Boronat, S. González, F. Illas, *Chem. Commun.* **2007**, 3371.
  - [30] B. Silvi, A. Savin, *Nature* **1994**, 371, 683.
  - [31] R. F. W. Bader, *Atoms in Molecules: A Quantum Theory*, Oxford University Press, Oxford, UK, **1990**.
-